Available online at www.sciencedirect.com

ScienceDirect

Procedia Structural Integrity 17 (2019) 957–964

Structural Integrity Procedia

www.elsevier.com/locate/procedia

ICSI 2019 The 3rd International Conference on Structural Integrity

An experimental study on the fracture behavior of different aluminium alloys subjected to ballistic impact

Pradipta Kumar Jena[a]*, K Siva Kumar[a], R. K. Mandal[b], A. K. Singh[a]

[a]*Defence Metallurgical Research Laboratory, Kanchanbagh, Hyderabad – 500 058, India*
Department of Metallurgical Engineering, IIT (BHU), Varanasi – 221005, India

Abstract

The present study describes and analyses the experimental results pertinent to the ballistic behaviour of six different series of commercially available aluminium alloys namely, AA 2024, AA 2519, AA 5059, AA5083, AA 6061 and AA 7017 plates. The aluminium alloy plates display large differences in static mechanical properties in terms of strength and ductility. The ballistic resistance of these plates is evaluated by impacting deformable projectiles at a velocity of 830 ± 10 m/s at a normal angle of attack. The results include the observation of the damage area at the front of the aluminium alloy plates. The microstructures and micro-hardness values along the projectile penetration path have been investigated to understand the material deformation behaviour. The adiabatic shear bands have been observed in all the aluminium alloys after post ballistic impacts. From the ballistic testing experiments, it is observed that the AA-7017 plates display higher ballistic resistance among the tested aluminium alloys. The ballistic performance of the aluminium alloy plates has been correlated with their respective mechanical properties and post ballistic microstructure.

Peer-review under responsibility of the ICSI 2019 organizers.

*Keywords:*Aluminium alloys; Mechanical property; Ballistic performance; Adiabatic shear bands

1. Introduction

Armour materials are used to provide protection against different threats in the battle field. In modern war

* Corresponding author. Tel.: +91-040-2458-6728; fax: +91-040-24344535.
*E-mail address:*pradipta@dmrl.drdo.in

2452-3216
Peer-review under responsibility of the ICSI 2019 organizers.
10.1016/j.prostr.2019.08.127

scenario combat vehicles require light weight armour structures with improved survivability to maintain mission performance. Aluminium alloys are preferred as potential light armoured material owing to their high strength-to-density ratio, good energy absorption capability, ease of manufacturing and excellent corrosion resistance properties. Aluminium alloys exhibit good resistance against small arms and fragmentation based threats. It has been reported by Übeyli et al. (2007) that the aluminium alloys can display equally good or even better ballistic resistance than the steels. For the past several decades, there has been a considerable amount of investigations devoted for the development of aluminium alloys as armour material in light weight armoured vehicles. Previous studies have explored the ballistic behaviour of different series of aluminium alloys such as Al-Cu base AA 2219-T351, AA 2519-T87, Al-Mg base 5083, Al-Si base 6061, 6063, 6070, Al-Zn-Mg base AA 7017, AA 7020, AA 7039, AA7055 and AA 7075. However, studies on the relative ballistic performance of different aluminium alloys have received less attention.

It has been shown by Dixit et al. (1995) that the ballistic resistance of metal plates depends primarily on their strength. In a previous study by Jena et al. (2010), it is observed that the relationship between ballistic performance and the target strength is not linear. In addition, ballistic behaviour at high strain rates is a complex process involving many material parameters like strength, hardness, ductility, toughness, strain hardening co-efficient etc. Materials with a balanced combination of strength and toughness may exhibit better ballistic resistance in comparison to those only having higher strength or toughness, Mondal et al. (2011). It is, therefore, of interest to investigate the ballistic performance of different aluminium alloys.

For armour application, it is necessary to study the different fracture mechanisms occurring during ballistic impact such as plugging, petalling, discing, spalling. It is also important to study the material adjacent to the penetration channel in order to understand the response of the material at high strain rates. Material behaviour during ballistic impact is a complex localised phenomenon which alters the microstructure of the material and its mechanical behaviour. Adiabatic heating associated inhomogeneous deformation in the form of adiabatic shear bands (ASBs) is another critical aspect leading to fracture during high strain rate deformation. Nature of ASBs in different aluminium alloys under ballistic impact has been presented in various studies. Previous studies indicate the importance of the post ballistic characterisation in understanding the ballistic behaviour of materials.

In the present work, the ballistic behaviour of six different series of commercially available aluminium alloys namely AA 2024, AA 2519, AA 5059, AA5083, AA 6061 and AA 7017 plates have been evaluated by impacting with 7.62 mm steel projectiles. The ballistic behaviour of the different aluminium alloy plates have been interpreted in terms of their mechanical properties. The changes in the microstructures, hardness values and damage patterns in post impact samples have also been studied.

2. Experimental procedure

The analysed chemical compositions of the studied alloys for the present investigation are given in Table 1. The alloys were received from Aleris International, (USA) in the form of 20 mm thick rolled plates. The microstructures were characterised by optical microscopy. The specimens were prepared following standard metallographic techniques used for aluminium and its alloys. Keller's reagent (5ml HNO_3, 3ml HCl, 2ml HF and 190 ml water) was used for etching of the samples.

The mechanical properties of the different aluminium alloy plates were evaluated using hardness, tensile and V-notch Charpy impact testing. The bulk hardness of the plates was measured using a Vicker's hardness tester at a load of 10 Kg. Hardness values reported in this study is the mean value of at least ten measurements. For tensile testing, cylindrical tensile specimens were machined from the rolling direction of the plates. It was evaluated at room temperature using an INSTRON 5500 testing machine at a crosshead speed of 1.0 mm min^{-1}. For each alloy, three tensile tests were carried out and an average values of yield strength (σ_{YS}), ultimate tensile strength (σ_{UTS}) and elongation (ε) are reported. The machining of the tensile samples and testing procedure were in accordance with ASTM E8-93. Standard Charpy V-notch impact specimens (CVN) of 10×10×55 mm size were machined as per the ASTM standards (E23-02a). The tests were carried out using a Tinius-Olsen impact testing instrument to find out the impact properties of the aluminium alloys. Following impact testing, topographical features of the fracture surface of the broken charpy samples of aluminium alloys were observed using a FEI scanning electron microscope (SEM).

The ballistic impact experiments were carried out in a small arms range. Samples of 200×200×20 mm size were

cut for ballistic testing. The ballistic samples were fastened tightly to a target holding fixture located at a distance of 15 m from the gun. The aluminium alloy plates were impacted by lead projectiles at 0° angle of impact. The hardness of the lead projectiles was measured to be around 25 HV (Vickers hardness number). The diameter of the projectile was 7.62mm. The velocities of all the ballistic tests were within range of 830 ± 10 m/s. The striking and residual velocities of the projectiles were measured using infra red light emitting diode photovoltaic cells. With proper gun alignment, it was assured that the centre-to-centre distance between any two impact craters on the target plates was at least three times the diameter of the projectile. A minimum of three shots were fired to each plate and three plates were ballistically evaluated for each aluminium alloy. A more detailed description of ballistic tests has been described elsewhere [Jena et al. (2010)].

The impacted aluminium alloy plates were cut into half across the craters and then subjected to standard metallographic procedure to reveal the post ballistic microstructures. The microstructure adjacent to the penetration channel was observed using optical microscope. The variation in hardness values adjacent to the penetration channel were measured using a Leica micro hardness tester at 50 gm load.

Table 1. Chemical compositions (wt.%) of different aluminium alloys

Material	Cu	Mg	Si	Mn	Fe	Ti	Cr	Zn	Al
AA 2024	4.05	1.43	0.43	0.38	0.32	0.017	0.1	--	Balance
AA 2519	5.5	0.3	0.23	0.4	0.3	--		0.1	Balance
AA 5059	0.2	5.6	0.3	1.0	0.4	0.2	0.2	0.6	Balance
AA5083	0.1	4.7	0.4	0.7	0.3	0.15	0.2	0.23	Balance
AA 6061	0.4	1.2	0.8	0.15	0.7	0.15	0.35	0.25	Balance
AA 7017	--	2.3	0.35	0.2	0.45	--	0.35	5.2	Balance

3. Results

The initial microstructures of the different aluminium alloy plates are given in Fig.1. The microstructures of the plates exhibit elongated grains along the rolling direction.

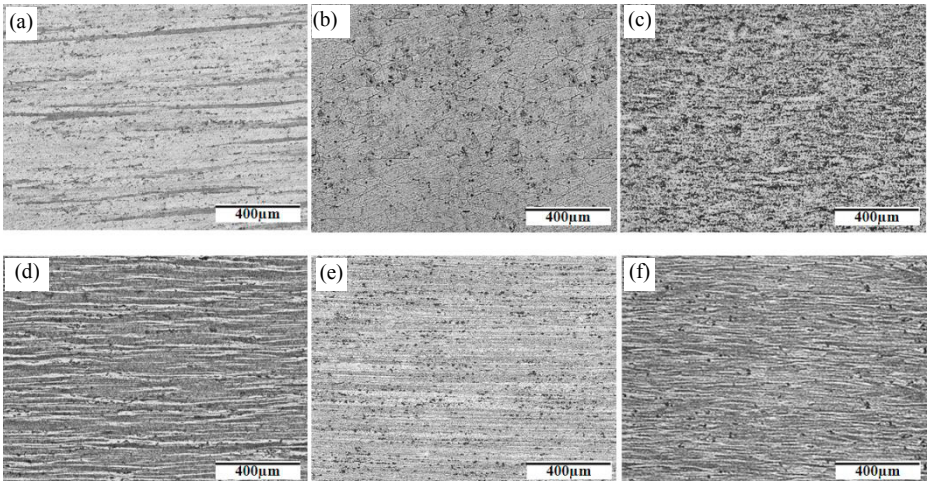

Fig. 1. Initial microstructures of the studied aluminium alloy plates taken along the longitudinal direction ; (a) AA 2024, (b) AA 2519, (c) AA 5059, (d) AA 5083, (e) AA 6061 and (f) AA 7017.

The representative engineering stress-strain and true stress-strain curves of the different aluminium alloy plates are displayed in Fig. 2 (a and b). The nature of the stress-strain curves of AA 2024, AA 2519, AA 6061 and AA7017 aluminium alloy plates displays typical nature of flow stress that increases continuously up to ultimate tensile strength. Serrated flow pattern was observed in the plastic deformation region of the stress-strain curves of AA 5059

and AA 5083 aluminium alloy plates. It is to be noted that the serrated flow pattern starts at some critical strain and not in the beginning of plastic deformation. Observation of serrated flow pattern in AA 5083 alloys has been reported in a previous investigation by Motsi et al., (2016). The mechanical properties of the different aluminium alloy plates are summarized in Table 2. The AA 7017 plate shows the highest hardness and tensile strength, whereas the AA 6061 plate displays lowest hardness and strength values. The AA 2024 alloy plate exhibits highest value of ductility measured in terms of total elongation to failure.

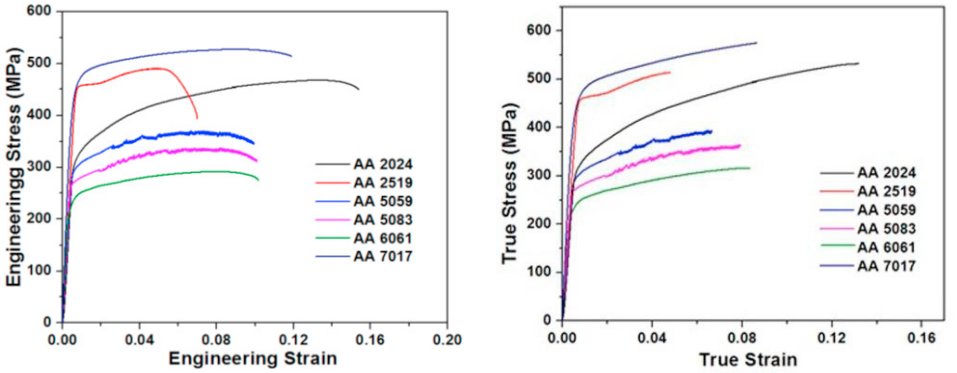

Fig. 2. (a) Engineering stress-strain and (b) True stress-strain curves of studied aluminium alloys.

Table 2. Mechanical properties of studied aluminium alloy plates.

Material	σ_{YS} (MPa)	σ_{UTS} (MPa)	Hardness (VHN)	% Elongation	CVN (J)
AA 2024	310	457	130	16.2	15
AA 2519	453	485	135	7.6	7
AA 5059	315	408	113	9.9	13
AA5083	279	346	107	10.1	14
AA 6061	250	294	87	10.4	17
AA 7017	437	513	160	11.4	9

The Charpy impact test results of different aluminium alloy plates are illustrated in Table 2. It can be noticed that the AA 6061 and AA 2519 plates display the highest (17 J) and lowest (7 J) impact energy values, respectively out of the studied alloys. The variations in fractographic features in the fracture surfaces of the broken Charpy impact specimens are depicted in Fig. 3. The fracture surfaces of all the aluminium alloy plates are predominantly dominated by dimples. Very fine and shallow dimples are observed in case of the fracture surface of AA 6061 samples whereas coarse dimples are seen in case of AA 2519 samples. On the other hand, a mixture of fine and coarse dimples is observed in the fracture surfaces of other studied aluminium alloys. Presence of intermetallic precipitates can be seen in the fracture surface of all the aluminium alloys.

From the ballistic testing, it is observed that all the different aluminium alloy plates are completely perforated by the projectile. The visual comparison of the different aluminium alloy plates after ballistic impact is exhibited in Fig. 4 (a). The damage mechanisms displayed by all the targets clearly indicate that the projectiles have pierced through the plates by causing ductile hole enlargement phenomenon. A close view of the front damage pattern elucidates that the material flows out to form perfect petalling damage pattern in the front side of the target plates (Fig 4 (b)). The residual velocity has been plotted against the tensile strength of the aluminium alloy target plates, (Fig. 5(a)). It can be seen that the residual velocity decreases with increase in tensile strength of the target plates. The kinetic energy absorbed by the different aluminium alloy target plates during ballistic testing is calculated by the following formula is shown in Fig 5 (b).

$$Eabs = ½ MV_s^2 – ½ MV_r^2 \quad (1)$$

Where Eabs = energy absorbed by the projectile, M = mass of the projectile, Vs =striking velocity of the projectile, Vr = residual velocity of the projectile. The alloy AA 7017 target plates exhibit highest energy absorption. At the

same time, the lowest energy absorption is observed in AA 6061 plates among the studied aluminium alloys. The impact craters are sectioned into two halves after ballistic testing and are shown in Fig. 6. There are no cracks observed visually in the crater region of any of the aluminium alloy plates.

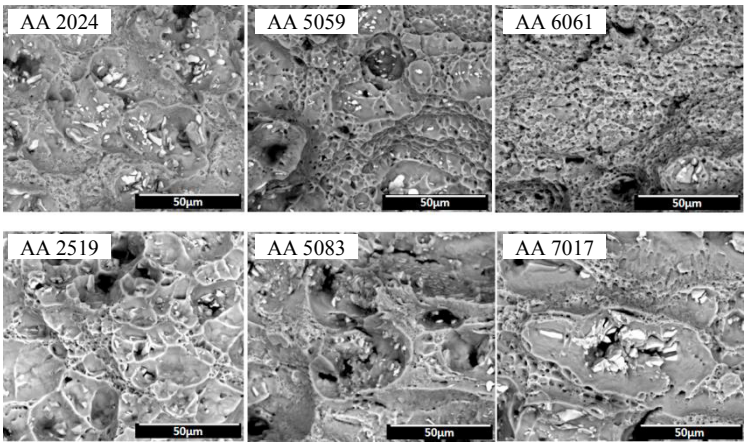

Fig. 3. Fractographs of Charpy impact fracture surfaces of different aluminium alloy plates.

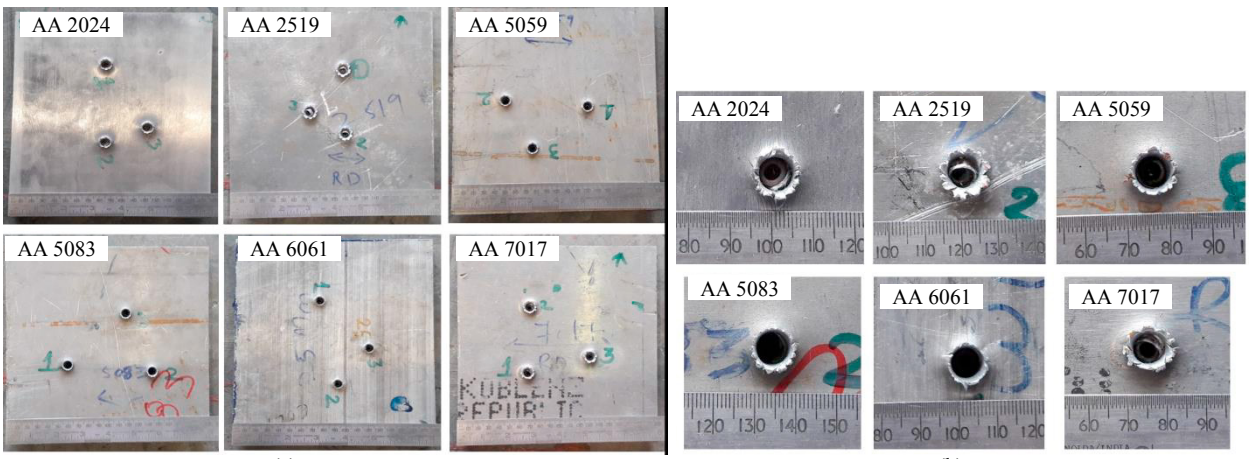

Fig. 4. (a) Front face of the aluminium alloy plates after ballistic impact and (b) close up view of the damage patterns.

The post ballistic microstructures of the aluminium alloy plates are illustrated in Fig.7. In all the aluminium alloy plates, material flow lines bend in the opposite direction of projectile motion along with large material deformation. Small cracks are detected in the crater of AA 2519 target plates. ASBs are seen in the crater region of all the aluminium alloy target plates. However, lesser ASBs are noticed in the crater of AA 6061 target plates. Micro-hardness measurements are taken at a load of 100 gm starting from close to the crater wall and gradually moving away. The variation in micro-hardness values in all the studied aluminium alloy target plates are shown in Fig. 8. In all the aluminium target plates, there is an initial rise in the hardness value and then it decreases with distance from crater wall.

4. Discussion

The alloys AA 2024, AA 2519, AA 6061 and AA 7017 belong to the series of heat treatable category. In contrast, AA 5059 and AA 5083 belong to the series of work hardenable aluminium alloys. The heat treatable aluminium alloys obtain their optimum properties through aging process where the formation of coherent

precipitates enhances the strength and hardness of the material. The AA 5059 and AA 5083 alloys achieve their properties through alloying elements and the application of strain-hardening by heavy rolling operation. The amount of alloying additions and morphology of precipitates play an important role in the strength and hardness of the aluminium alloys. From Table 1, it can be noticed that the AA 7017 alloy has the maximum amount of alloying elements in its composition. This explains the observation of the highest strength and hardness in AA 7017 alloy. The AA 6061 has the lowest amount of alloying elements in its composition and hence displays the lowest strength and hardness values. There is a limit up to which the strength and hardness can be increased by strain hardening process. Hence, the AA 5059 and AA 5083 alloys exhibit lower strength and hardness in comparison to AA 2024, AA 2519 and AA 7017. It has been reported that heat treatable aluminium alloys demonstrate higher strength and hardness than those of the work hardening aluminium alloys, Crouch, (2016).

Charpy impact energy values give a good indication of the resistance to failure of a material to a sudden applied force and are generally correlated with the ballistic behaviour of materials. The dimple like morphology observed in the fracture surfaces of broken Charpy impact samples of all the studied aluminium alloys clearly indicates a ductile failure mode. Ductile mode of failure implies extensive plastic deformation and energy absorption before fracture and is a desirable criterion for armour materials. The difference in impact energy of the different aluminium alloys can be explained from their respective fracture surfaces (Fig. 3). The fine and shallow dimples in AA 6061 plates facilitate in absorbing the kinetic energy in an efficient manner. Hence, AA 6061 plates exhibit the highest Charpy impact values among the studied aluminium alloys. The coarse dimples seen in the fracture surface of AA 2519 plates decreases the energy absorption and hence a reduction in the Charpy impact values.

The energy absorption by different aluminium alloy plates during ballistic impact can be depicted from the post ballistic microstructural observations. The target material tries to absorb the kinetic energy from projectile during ballistic impact. This results in the observation of deformed and distorted material flow lines adjacent to the crater region.

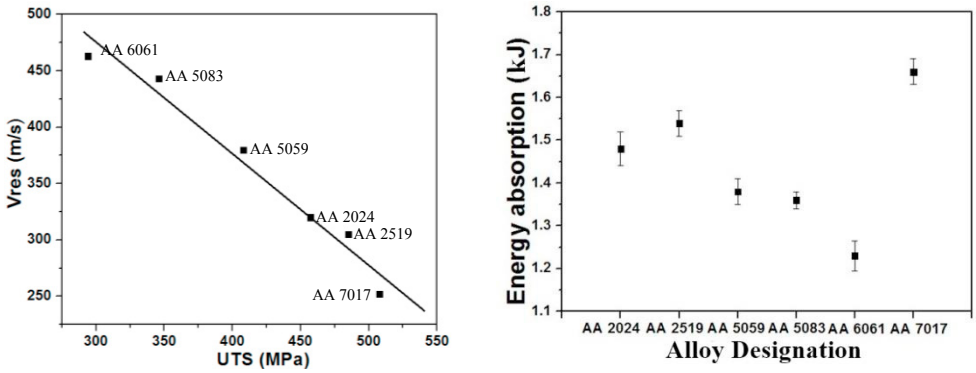

Fig. 5. (a) Residual velocity (Vres) with UTS of the target plates, (b) Kinetic energy absorption by different aluminium target plates.

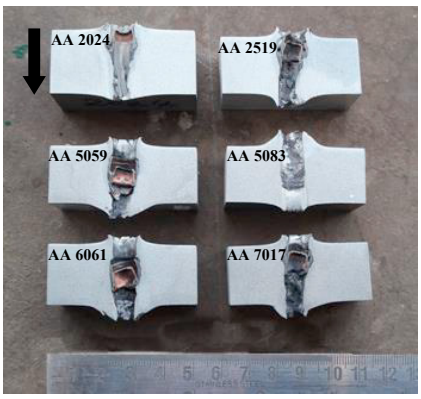

Fig. 6: Half section views of the impacted craters after ballistic testing. Arrow mark indicates the projectile penetration direction.

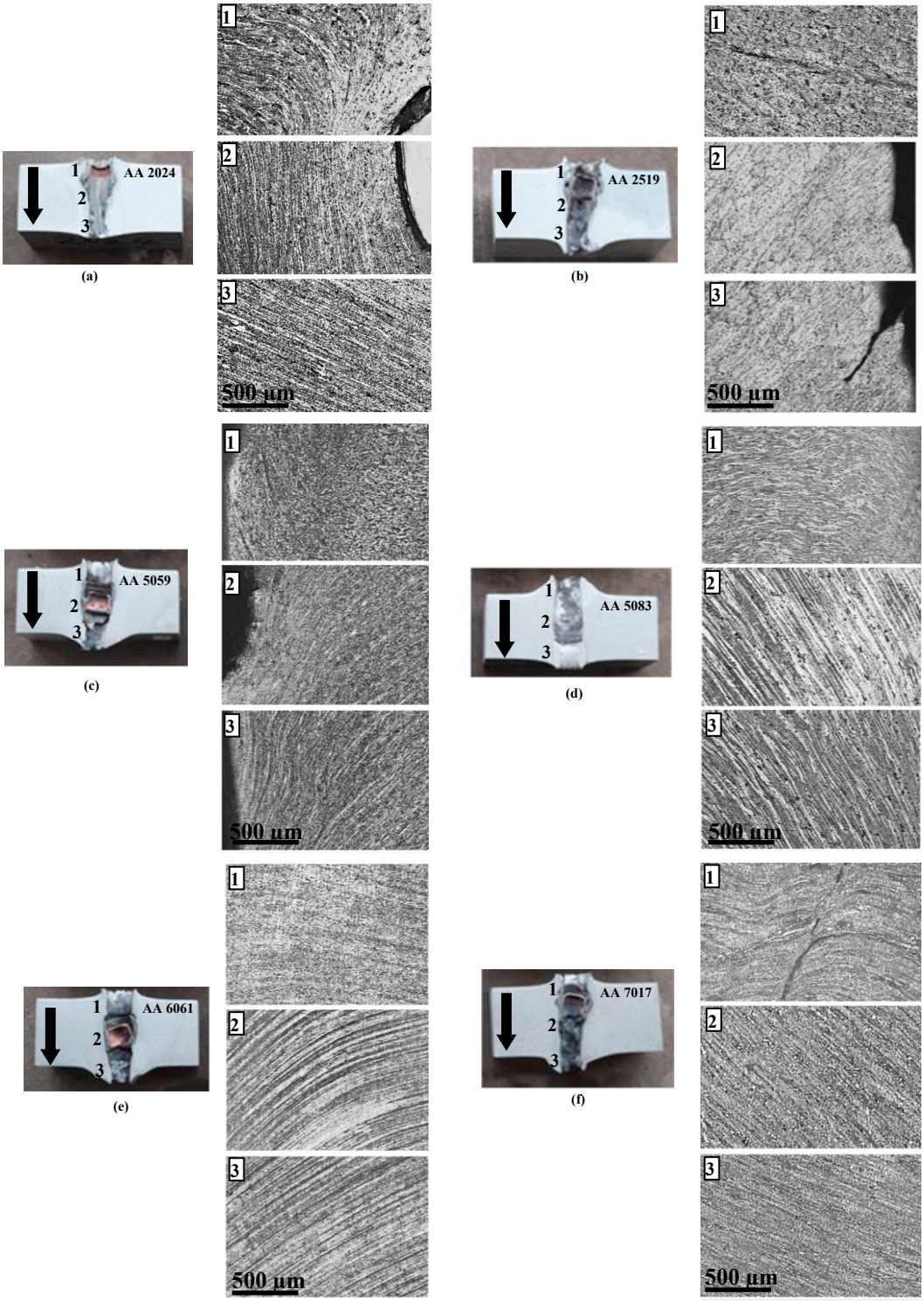

Fig. 7. Post ballistic microstructure adjacent to the crater wall of (a) AA 2024 (b) AA 2519 (c) AA 5059 (d) AA 5083(e) AA 6061 (f) AA 7017 target plates. Arrow mark indicates the projectile penetration direction. The numbers in the microstructure indicate the corresponding region in the crater wall.

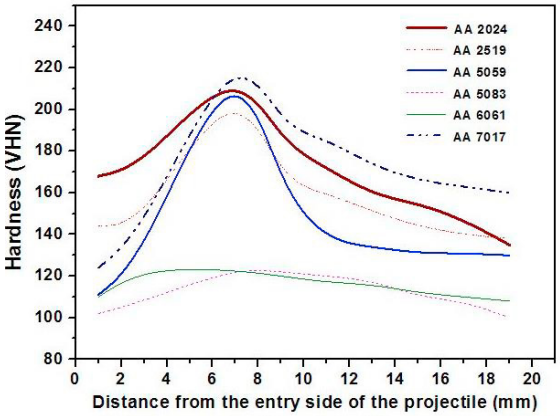

Fig. 8. Post ballistic micro-hardness measurements adjacent to the crater wall of different aluminium alloy plates.

High Charpy impact energy assists in dissipation of the impact energy over a larger volume of the material and hence a homogeneous deformation is observed. However, at low Charpy impact energy value, an in-homogeneity in deformation is observed. This causes the formation of ASBs. Shear band is formed due to thermo-mechanical instability during projectile impact, Timothy (1987). The cracks observed in the post ballistic microstructure of AA 2519 craters can be correlated to its lowest Charpy impact values. The hardness values adjacent to the crater wall indicate the extent of deformation during ballistic impact. The variation in hardness adjacent to the crater region is a result of annealing and strain hardening caused by projectile impact, Jena et al. (2017).

Ballistic resistance increases with increase in material properties like strength and hardness. Consequently, the AA 7017 target plates display the best ballistic performance owing to its highest strength and hardness values among the studied aluminium alloys. The results are in line with the previous studies, Borvik et al. (2009).

5. Conclusions

The AA 7017 alloy exhibits the best ballistic performance among the studied materials. Ballistic penetration resistance of the present alloys is in accordance with their strength and hardness values. ASBs are observed at the target projectile interface in all the studied aluminium alloys. Formation of ASBs can be correlated with the Charpy impact energy value of the aluminium plates.

Acknowledgement

The authors wish to acknowledge DRDO, Government of India for financial support and The Director, DMRL for his encouragements to present this work at ICSI 2019 conference.

References

Borvik ,T., Dey, S., Clausen, A. H., 2009. Perforation resistance of five different high strength steel plates subjected to small arms projectiles. International Journal of Impact Engineering 36(7), 948–964.

Crouch, I.G., 2016. The Science of Armour Materials, Woodhead Publishing, Elsevier Science and Technology, pp. 1-54.

Dikshit, S. N., Kutumbarao, V. V., Sundararajan, G., 1995. The influence of plate hardness on the ballistic penetration of thick steel plates. International Journal of Impact Engineering 16(2), 293–320.

Jena, P. K., Mishra, B., RameshBabu, M., Babu, A., Singh, A.K., Sivakumar, K., Bhat, T. B., 2010. Effect of heat treatment on mechanical and ballistic properties of a high strength armour steel. International Journal of Impact Engineering 37, 242-249.

Jena, P.K., Savio, S.G., SivaKumar, K., Madhu, V., Mandal, R. K., Singh, A. K., 2017. An experimental study on the deformation behavior of Aluminium armour plates impacted by two different non-deformable projectiles. Procedia Engineering 173, 222 -229.

Mondal, C., Mishra, B., Jena, P. K., SivaKumar, K., Bhat, T. B., 2011. Effect of heat treatment on the behaviour of an AA7055 aluminum alloy during ballistic impact. International Journal of Impact Engineering 38, 745-754.

Motsi, G. T., Shongwe, M. B., Sono T. J.,Olubambi, P. A., 2016. Anisotropic behaviour studies of aluminium alloy 5083-H0 using a micro-tensile test stage in a FEG-SEM. Material Science and Engineering A 656, 266-274.

Timothy, S.P., 1987. The structure of adiabatic shear bands in metals: A critical review. Acta Metallurgica 35(2) 301-306.

Übeyli, M., Yıldırım, R. O., Ögel, B., 2007. On the comparison of the ballistic performance of steel and laminated composite armors. Materials and Design 28(4), 1257–1262.